Synthesis of Bamboo-Based Activated Carbons with Super-High Specific Surface Area for Hydrogen Storage

Weigang Zhao,[a] Lu Luo,[a] Hongyan Wang,[b] and Mizi Fan [c,*]

Activated carbons (ACs) were developed from the agricultural by-products of moso bamboo by pyrolysis carbonization and the KOH activation process. N_2 adsorption-desorption at 77 K, thermogravimetric analysis (TG), X-ray photoelectron spectrometry (XPS), element analysis (EA), X-ray diffraction (XRD), scanning electron microscopy (SEM), high-resolution transmission electron microscopy (HRTEM), and Fourier transform infrared spectroscopy (FTIR) were used to investigate the synthesis process, the impact of the weight ratio of KOH/bamboo charcoal (BC), and the characteristics of the bamboo charcoal and ACs produced. The results showed that the developed bamboo ACs achieved surface areas (S_{BET}) as high as 3208 m^2/g and micropores volumes (V_{DR}) as high as 1.01 cm^3/g. The carbonation and activation of the bamboo resulted in the enhancement of the microstructure of the bamboo ACs, and hence improvements in the sorption behavior and storage capacity. The highest hydrogen storage capacities achieved were 6.6 wt.% at 4 MPa and 2.74 wt.% at 1 bar, both at 77 K, which were much higher than those of a well-known commercial activated carbon.

Keywords: Bamboo; Activated carbon; Hydrogen storage; Microstructures; Storage capacity

Contact information: a: College of Material Engineering, Fujian Agriculture and Forestry University, NO 15 Shangxiadian Road, Fuzhou 350002, PR China; b: Key Laboratory of Bamboo Research, Zhejiang Forestry Academy, Liuxia Xiaoheshan, Hangzhou 210037, PR China; c: College of Engineering, Design, and Physical Sciences, Brunel University, Uxbridge UB8 3PH, United Kingdom;
** Corresponding author: weigang-zhao@hotmail.com*

INTRODUCTION

Energy security and climate change are two of the most important global problems in the twenty-first century, and technological solutions are believed to be necessary for resolving these problems. Although hydrogen is not currently a widely used fuel, it holds great potential to be a means of providing clean, safe, affordable, and secure energy in the future because it is a renewable energy source that generates no carbon emissions (Marbán and Valdés-Solís 2007). Hydrogen can be used not only as fuel for cars, light trucks, ships, airplanes, and trains, but also to generate electricity for heating and manufacturing (Zhao *et al.* 2012b, 2013). One of the greatest problems connected with hydrogen is the method of its storage. The US Department of Energy (DOE) set new goals in 2009 for automotive applications of hydrogen: reversibility, a gravimetric density of approximately 6 wt.%, and consideration of the entire storage system (Zhao *et al.* 2012a). Currently, the traditional methods of storage include either compressing or liquefying hydrogen, which are limited by being highly energy demanding, inefficient, and relatively unsafe (Xiao *et al.* 2014). Meanwhile, there has been a lot of research related to hydrogen adsorbed by metal hydride materials (Rango *et al.* 2016), carbon materials (Zhao *et al.* 2012b, 2013; Sethia and Sayari 2016), and MOF (Ren *et al.* 2015) by physisorption or chemisorption. Among others,

activated carbon (AC) is one of the most attractive hydrogen storage carriers because of its advantages of being reversible, having a high specific surface area and pore microstructure, being light weight (low density), being stable for large scale production, and having fast kinetics (Zhao *et al.* 2016).

The excellent adsorption capacity and versatility of AC makes it an effective option for gas phase, drinking water, and wastewater treatment (Liu *et al.* 2010; Wang 2012; Wang *et al.* 2013, 2015; Huang *et al.* 2014, 2015; Odoemelam *et al.* 2014; Wu *et al.* 2015). Any carbonaceous materials having a high carbon content and moderate inorganic contents, such as coal, peat, polymeric materials, wood, bamboo, and various agricultural by-products, can be used as the carbon precursor (Marsh and Rodríguez-Reinoso 2006). Currently, there are many studies on the development of low-cost adsorbents, *e.g.*, biomass materials derived from agricultural and forestry by-products (Vamvuka *et al.* 2006). Bamboo is one of the most attractive natural resources that can be found in Asia, and it is especially abundant in China, Thailand, and Vietnam. China has the richest bamboo resources in the world, with over 500 species in 39 genera and is a center of the origin and distribution of bamboo (Zhou *et al.* 2011). Bamboo is the fastest growing, highest-yielding renewable natural resource that is widely used as a building, furniture, papermaking, and clothing material (Shen *et al.* 2004; Tang and Smith 2014; Li *et al.* 2015). Still, every year, more than 50,000 tons of bamboo scaffolding ends up in landfills (Koo *et al.* 2015). The possibility of preparing activated carbons (AC) from bamboo by physical and/or chemical activation has recently been investigated, but they have been mainly used as adsorbents in wastewater treatment (Ouyang *et al.* 2014; Shang *et al.* 2014; Zhang *et al.* 2014). Efficient bamboo utilization, in particular for high value-added applications, has yet to be explored.

This research presents the development of bamboo-activated carbons, using KOH as the activation agent for hydrogen storage, which would not only generate value-added products from this agricultural residue, but also offer a potentially cost-effective alternative to commercial ACs. The synthesis process of bamboo-derived activated carbons, the impact of the weight ratio of KOH/bamboo charcoal (BC), and the characterizations of the BC and ACs produced were investigated. The developed ACs possessed much higher hydrogen storage capacities than the well-known commercial activated carbon Maxsorb-3, which has not been previously reported.

EXPERIMENTAL

Preparation of Activated Carbons from Bamboo

The moso bamboo culms (*Phyllostachys edulis*) that were selected as a char precursor were obtained from the Fujian Province, China. All reagents were of analytical grade and used without further purification or treatment.

Bamboo culms with dimensions of 40 x 20 x 5 mm were prepared in a high-speed rotary cutting mill and then put into a horizontal tubular furnace under a pure nitrogen environment and subjected to a gradual increase in temperature (5 °C/min) from room temperature to 650 °C, at which they were kept for 1 h. The flow rate of the nitrogen was 200 mL/min. After the furnace had been cooled down to room temperature under nitrogen atmosphere, the bamboo charcoal (BC) was finally produced.

The BC was ground and sieved in order to generate a uniform powder with particle sizes of 100 to 200 μm. KOH in the form of pellets was then physically mixed with the BC powder at various designed weight ratios (W) of KOH/BC. The resultant mixture was then

introduced into a nickel crucible and heat-treated in a muffle furnace (KDF, 80-plus) at a constant heating rate (3 °C/min) up to the final activation temperature (T=800 °C), which was maintained for 2 h. The crucible was then allowed to cool down to room temperature. The whole process was conducted under a stream of nitrogen with a flow rate of 300 mL/min. Finally, the activated product was washed, first with distilled water (for the recovery of the rudimentary KOH), then with HCl (1 M), and finally, with distilled water again until the pH of the rinse had stabilized. After being dried in an oven for 12 h, a very pure activated carbon (AC) material was obtained. The developed AC was stored in a vacuum desiccator for subsequent pore texture characterization and hydrogen adsorption experiments. Figure 1 shows the schematic of the preparation process.

All the ACs prepared were labeled as ACx. In this nomenclature, the x at the end corresponds to the different weight ratios. For example, AC4 meant that the weight ratio of the KOH/BC was 4.

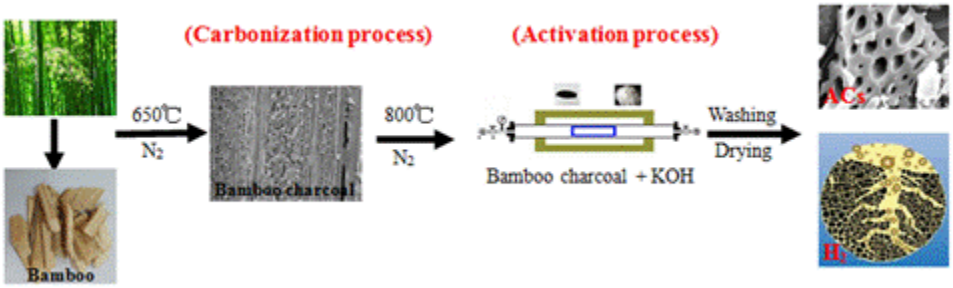

Fig. 1. Schematic of the preparation process

Physicochemical Characterization of the Materials

The structural characterization was performed by means of X-ray diffraction (XRD) using a Bruker D8 Advance instrument from USA (Cu-K, Bragg-Brentano Geometry). The morphologies were studied by means of scanning transmission electron microscopy (SEM) observations (FEG SEM Hitachi S 3400, Japan) and high resolution transmission electronic microscopy (HRTEM, JEOL JEM-2100 at an accelerating voltage of 200 kV). The elemental analysis (EA) was determined using a Vario EL-III CHNSO elemental analyzer (Germany), and using an X-ray photoelectron spectrometer (XPS) (SPECS XPS system, Germany) operated at 150 W with Al-Kα radiation. The Fourier transform infrared spectra (FTIR) measurements were carried out using a VERTEX 70 instrument from Bruker (USA). The TG curves representing the carbonization and activation processes at the weight ratio (W=4), were obtained by means of thermogravimetric analyses (TGA, SDT-Q600, NETZSCH, Germany). The samples were heated from room temperature to the final temperature of 1000 °C at a rate of 10 °C/min under an atmosphere of N_2 maintained at a flow rate of 20 mL/min.

The nitrogen adsorption-desorption isotherms were measured using an automatic apparatus (Micromeritics ASAP 2020, USA) operated at 77 K. The details can be found by consulting the authors' previous studies (Zhao *et al.* 2012b, 2013). Prior to the adsorption experiments, the samples were degassed for 24 h under a vacuum at 563 K. The N_2 adsorption data were processed to generate the following: (i) the surface area, S_{BET}, by the BET calculation method (Brunauer *et al.* 1938); (ii) the micropore volume, V_{DR}, according to the Dubinin-Radushkevich (DR) method (Dubinin and Polstyanov 1989); and (iii) the total pore volume, $V_{0.99}$, defined as the volume of liquid nitrogen corresponding to the amount adsorbed at the relative pressure P/P_0 = 0.99 (Gregg and Sing 1982). The average micropore diameter, L_0 (Stoeckli *et al.* 2002), and the pore size distributions, PSD, were

also calculated by the application of density functional theory (DFT) (Tarazona 1995). EA represented the characteristic adsorption energy of nitrogen and was derived from the corresponding adsorption isotherms at 77 K by applying the DR method (Dubinin and Polstyanov 1989).

Measurement of the Hydrogen Storage Capacities at 77 K

The hydrogen storage capacities both at low pressure and high pressure at 77 K were determined. The ASAP 2020 HD88 from Micromeritics in USA was used for the low-pressure measurements (up to 1 bar) and the gravimetric analyzer HPVA-100 (VTI Corporation of TA Instruments, USA) was used for the high-pressure measurements (up to 8 MPa). For both sets of measurements, the samples were outgassed under a primary vacuum at 350 °C for 24 h before any sorption measurements were taken.

RESULTS AND DISCUSSION

Carbonation and Activation Process

The carbonization and activation temperatures may influence the pore textures of the ACs, depending on the precursors used (Li *et al.* 2008; Okieimen and Ogbeide 2009). The TG was used in this study to estimate the temperature of carbonization and the activation process for ACs from bamboo. It was apparent that the TG curve of the carbonization process presented a distinct weight loss, starting from 240 °C and ending at 600 °C (Fig. 2), that was primarily due to the release of H_2O, CO_2, and CO resulting from the escape of H and O atoms in the bamboo, which left porous tunnels in the carbonized bamboo (BC). Hence, the yield of the bamboo carbonization was 24.3%, which was similar to that of most of the bamboo charcoal prepared in previous studies (Choy *et al.* 2005; Huang *et al.* 2014).

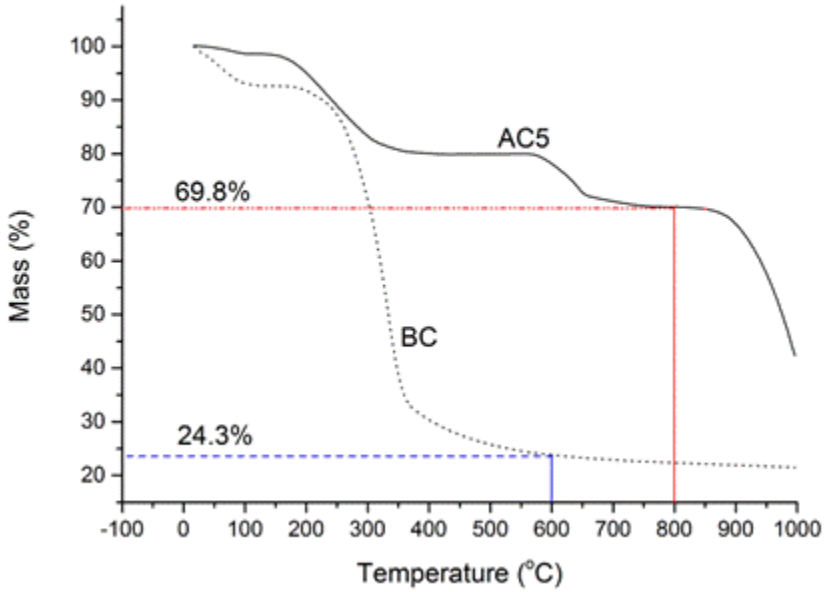

Fig. 2. TG curves of bamboo under N_2 atmosphere (dotted line) and AC5 under N_2 atmosphere (solid line)

Figure 2 also shows the TG curve of the activation process up to 1000 °C for the mixture of pre-carbonized bamboo (BC) and KOH at the weight ratio of 5. The weight loss at low temperatures (< 350 °C) may have been due to the dehydration of the activation agent KOH, which was followed by a structural transformation. There was almost a plateau between 350 and 550 °C, indicating that there may have been no activation reaction. The temperature ranges from 550 to 750 °C corresponded to a sharp mass loss, which may be attributed to the C-KOH reaction, which led to the development of pore systems. Overheating can happen when the activation temperature is higher than 850 °C, and this is reflected in the considerable weight loss (*i.e.*, the great mass reduction) that occurred (Wang *et al.* 2014). Therefore, it could be inferred that the most favorable activation temperature should be in the range of 750 to 850 °C. The activation temperature used in this study was 800 °C, corresponding to a yield of 69.8%. Thus, the total carbon yield for the AC5 samples was approximately 17%.

Elemental Composition Analysis

XPS analysis was carried out to investigate the effects of the KOH activation process on the elemental composition of the carbonized materials (BC) and activated carbon (AC5) (Fig. 3). The three characteristic peaks of C1s (284.62 eV), O1s (533.23eV), and N1s (399.78eV) can be observed in the full XPS spectra. As can be seen, the N1s peaks for both the BC and AC5 were very weak. In addition, the KOH activation process removed area from the O1s and added area to the C1s peaks. The reduction in the O1s peaks area may have been due to the reaction between K and C and the removal of CO and CO_2; however, the increase in C1s was due to the increase in the quantity of C-C bonds (Xiao *et al.* 2014; Heo and Park 2015). The atomic percentages (wt.%) of C, O, and N were calculated to be 81.35%, 15.34%, and 0.70% for the BC and 94.60%, 5.15%, and 0.26% for the AC5, respectively, which confirmed the EA results shown in Table 1.

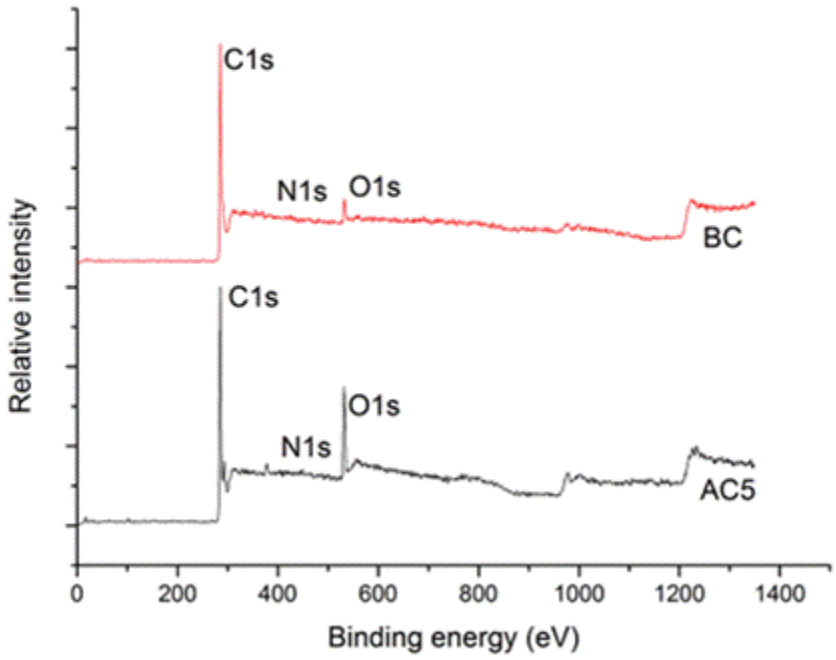

Fig. 3. XPS spectra of sample BC and AC5

Table 1. Chemical Analysis of Bamboo and Bamboo-derived Products

#AC	N (wt.%)	C (wt.%)	O (wt.%)	H (wt.%)	S (wt.%)
Bamboo	<0.3	46.12	33.22	6.29	<0.5
BC	0.48	77.10	14.00	2.62	<0.5
AC5	<0.3	90.11	5.99	0.52	<0.5

Surface Chemistry of Bamboo ACs

The results of the FTIR study on the bamboo, bamboo charcoal, and activated carbon samples are presented and compared. Figure 4 shows the FTIR spectra in the mid-infrared region between 400 and 4000 cm^{-1}. It is apparent that there were chemical changes due to the carbonization and activation of the bamboo. Judging from the peak position and peak shape, the broad band found at 3400 cm^{-1} could generally be attributed to the O-H stretching vibration of hydroxyl and carboxyl, whereas the magnitude of the characteristic peaks of the methylene C-H asymmetric vibrations were located at 2922 and 2852 cm^{-1}. Meanwhile, significant differences were observed in the range of 1000 to 1450 cm^{-1}, corresponding to the numerous residual hydroxyl groups could be attributed to the O-H bending vibration and the C-O (hydroxyl, ester, or ether) stretching vibrations. The two additional bands at 1600 cm^{-1} and 1720 cm^{-1}, respectively, were due to the stretching vibration of the carboxyl groups of the C=O and C=C bonds. It was also evident that the bond at 1118 cm^{-1}, corresponding to the asymmetric stretching vibrations of the C-O and C–N bonds for the bamboo sample, was reduced following carbonation, and could not be found after the activation process. The significant absorption peak at 1450 cm^{-1} was caused by the aromatic C–H out-of-plane bending vibrations. Having stated the above, the carbonization and activation processes had significant effects on the surface properties of the activated carbon materials due to their destruction of heteroatoms and functional groups, which led to the reduction and even disappearance of those peaks after carbonation. These results were in good agreement with the results of the XPS and EA analysis.

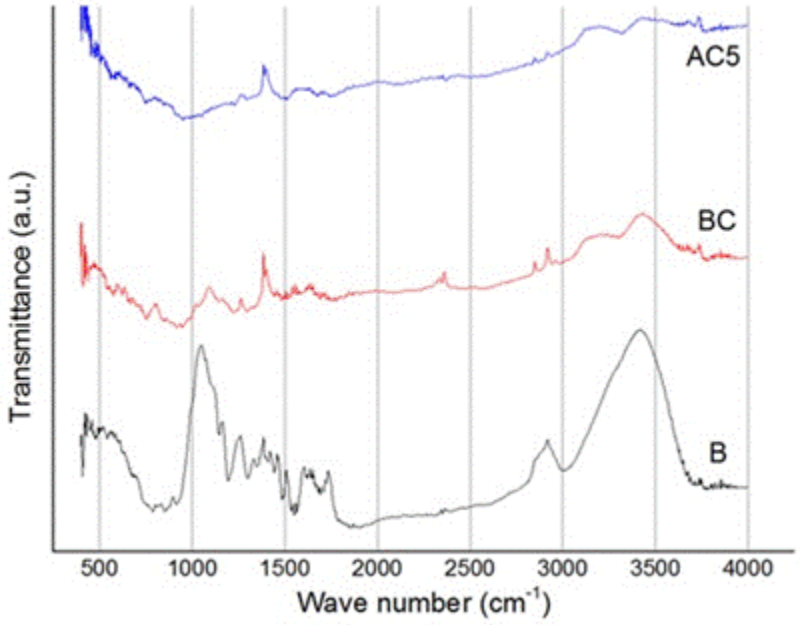

Fig. 4. FTIR spectra of (a) bamboo, (b) BC sample, and (c) AC5

Microstructure of Bamboo ACs

Aspects of the bamboo ACs microstructure are shown in Fig. 5.

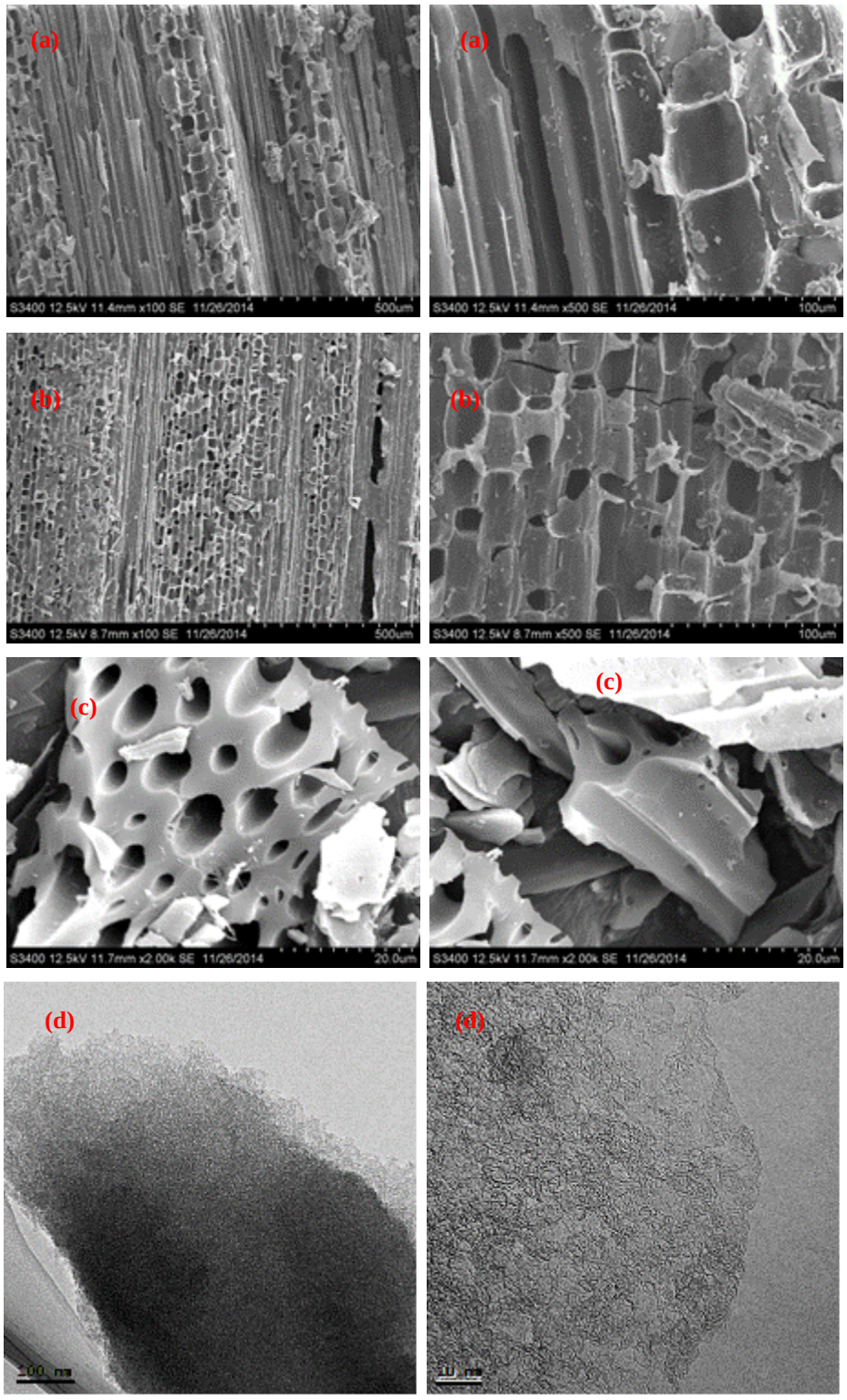

Fig. 5. (a) SEM image of the bamboo in the longitudinal direction, (b) SEM image of the BC sample in the longitudinal direction, (c) SEM image of the AC5 sample, and (d) HR-TEM image of the AC5 sample.

A comparison of the microstructures of the bamboo, BC, and the derived AC (for example, AC5) showed that after the carbonization at 650 °C, the BC maintained the structural characteristics of the original bamboo in terms of texture (Fig. 5b), such as those of the bamboo fibers and parenchyma cells (Fig. 5a), while more well-developed large, regular, and neatly arranged pores, measuring less than 5 μm, could be observed in the longitudinal section of the carbonized bamboo. During the activation with the KOH/C ratio of 5 at 800 °C, while these large macropores oriented parallel to the fibers were retained. This pore structure was favorable for the diffusion of H_2, and some nanosized pores may have also developed, as was observed on the surface of the AC sample. It was also considered that a large number of micropores and mesopores could have developed, as a very high surface area (3208 m^2/g) of this activated carbon was obtained from the N_2 adsorption and desorption; these pores were not visible on this SEM image because of their small size. The HRTEM images displayed in Fig. 5d further show that the AC5sample was rich with a highly microporous structure.

The carbonization may also have resulted in changes to the crystallinity of the bamboo ACs (Fig. 6). The XRD patterns of the BC and ACs at various values of *W* showed that the BC without KOH treatment had a typical amorphous graphite crystal structure, which was confirmed by the broad peaks appearing at approximately 2 theta = 24 (002) and 44 (101). After the KOH activation, both the peaks at 002 and 101 became less and less significant with the increase in *W*, and for sample AC5, they even totally disappeared. This could have been due to the breakdown of the hexagonal symmetry of the graphite lattice during the activation process by KOH, leading to defects in the lattice in the form of layer structure defects caused by K intercalation from the graphite crystalloids and the evaporation of C. The amount of K intercalation into the graphite crystalloids increased with the weight ratio of the KOH/BC (Xiao *et al.* 2014).

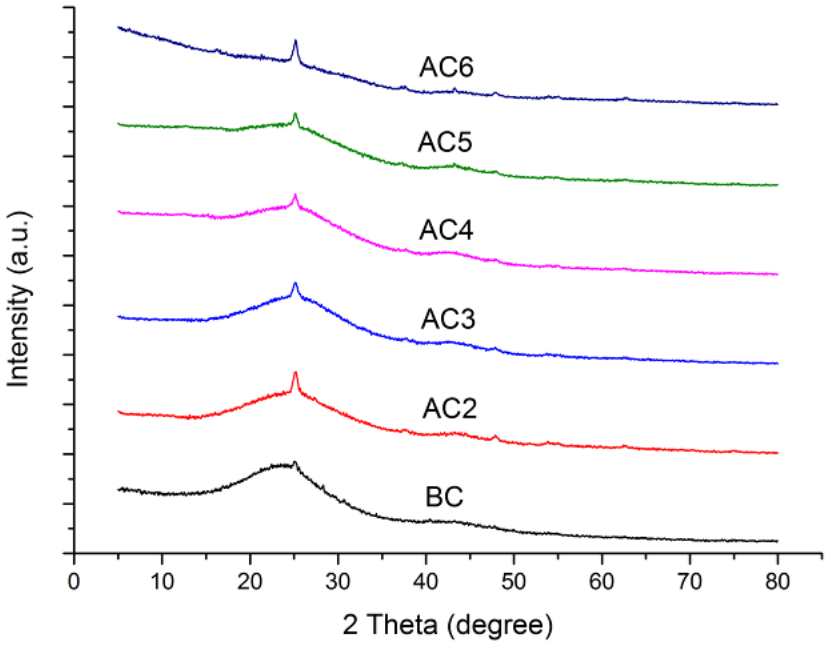

Fig. 6. XRD patterns of the BC and all the AC samples

N_2 Adsorption-Desorption Analysis

The textural characteristics reflected the N_2 adsorption-desorption at 77 K for the BC and all ACs, and the results are listed in Table 2. The BC presented a very low S_{BET} (337 m^2/g), which was reasonably comparable to those of other bamboo charcoals as reported previously (Wang *et al.* 2008). During the activation process, the redox reactions between the potassium compounds and carbon can result in an increase in the value of the specific surface area. When the weight ratio, *W*, was increased from 2 to 6, the S_{BET} increased from 1767 to 3208 m^2/g, the V_{DR} increased from 0.63 to 1.01 cm^3/g, and the $V_{0.99}$ increased from 0.9 to 1.75 cm^3/g. The ratio $V_{DR}/V_{0.99}$ was used to investigate the proportion of microporosity to total porosity. It was found that the developed ACs were essentially microporous, as the $V_{DR}/V_{0.99}$ varied from 53 to 70%. The average micropore diameter (L_0) was found to be in the range of 1.08 to 1.65 nm.

The weight ratio, *W*, has been found in previous studies to be the most important parameter in the KOH chemical activation process (Lillo-Ródenas *et al*. 2003; Zhao *et al*. 2012b). It is interesting that the AC5 sample achieved the highest S_{BET} and V_{DR}, and further increases in *W* to 6 resulted in decreases in both the S_{BET} and V_{DR}, even though the $V_{0.99}$ increased from 1.75 to 1.85 cm^3/g. This also indicated that the optimum *W* may change with the precursors used. This could be explained by the fact that during KOH activation, the formation of mesopores and pore widening are two main mechanisms of the development of porosity, and in general the process of pore widening occurred at high *W*s, which may damage the pores structure.

Table 2. Textural Characteristics of Bamboo ACs

#AC	W	S_{BET} (m^2/g)	$V_{0.99}$ (cm^3/g)	V_{DR} (cm^3/g)	*E*a (kJ/mol)	L_o (nm)	$V_{DR}/V_{0.99}$ (cm^3/g)	V_{meso} (cm^3/g)	H_2 uptake (wt.%)	
									1 bar	4 MPa
BC	0	337	0.14	N	N	N	N	N	0.86	1.2
AC2	2	1767	0.90	0.63	21.39	1.08	0.70	0.27	2.20	4.4
AC3	3	2559	1.25	0.85	20.19	1.23	0.68	0.40	2.74	5.8
AC4	4	3148	1.60	0.98	19.03	1.42	0.61	0.62	2.67	6.5
AC5	5	3208	1.75	1.01	18.19	1.59	0.58	0.74	2.58	6.6
AC6	6	2914	1.85	0.99	17.95	1.65	0.53	0.86	2.50	6.5

Figure 7 shows the N_2 adsorption and desorption isotherms at 77 K consisting of both linear and logarithmic patterns. The BC and all AC samples presented type I isotherms according to the IUPAC classification. The BC sample exhibited the lowest amount of adsorbed nitrogen. When the *W* value was increased, the amount of nitrogen adsorbed increased and showed a more extensive widening isotherm 'knee' at a low relative pressure. It is well known that the sorption behavior at low pressures corresponds to nitrogen adsorption in the micropores, where a much steeper increase means more micropores. Accordingly, as the *W* increased, the knee of the isotherm widened, indicating both the broadening of the micropore width and development of the mesoporosity. As the pressure increased, all the isotherms reached a plateau where there was no hysteresis cycle, even for the highest apparent surface area measured in this study (3208 m^2/g). The PSD was calculated using computer software by application of density functional theory (DFT) (Fig. 8). The result reinforced the aforementioned finding that the micropores were the major component of the AC structure, coexisting with a few mesopores. Increasing the *W* increased the micropore volume but also the fraction of larger pores.

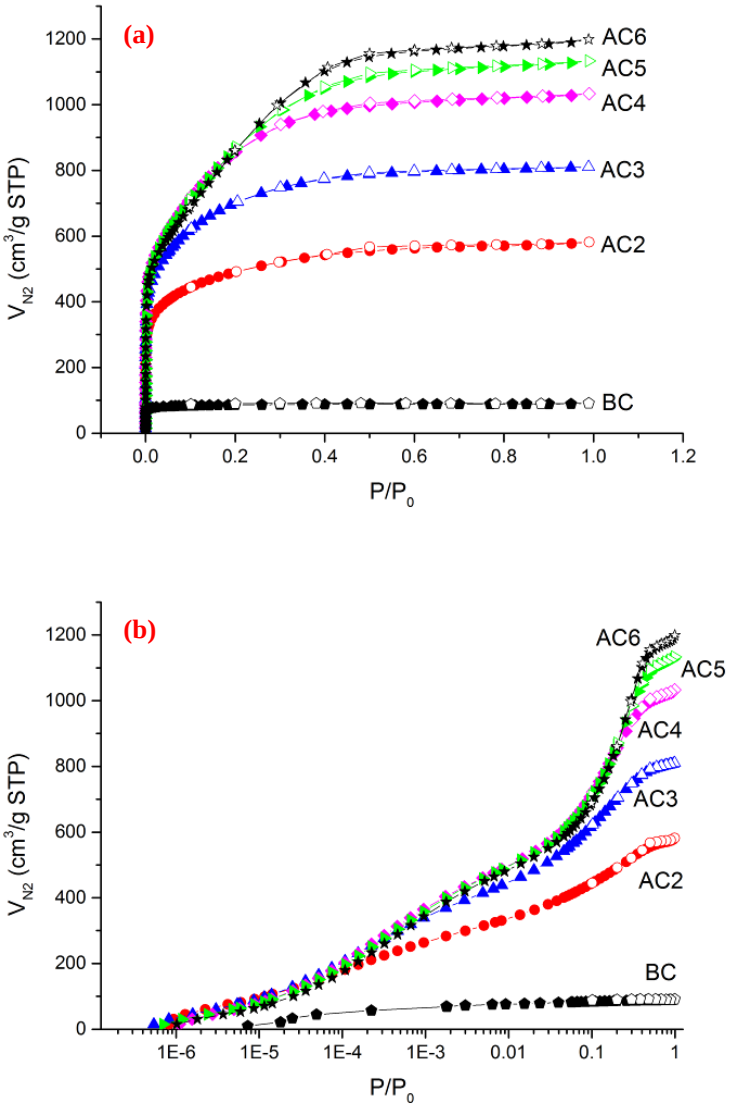

Fig. 7. N_2 adsorption (solid symbols) and desorption (hollow symbols) isotherms on both (a) linear and (b) logarithmic scales

Hydrogen Storage Performance

The hydrogen adsorption isotherms up to 1 bar and up to 8 MPa of the BC and ACs are given in Fig. 9, and the hydrogen storage capacities are listed in Table 2. There was no hysteresis cycle. For low pressures up to 1 bar, the isotherms increased continuously, as shown in Fig. 9a. Meanwhile, it is clearly shown that under high pressure (8 MPa), a clear plateau can be found for all the isotherms, as shown in Fig. 9b. The maximum hydrogen storage capacities of the BC were 0.86 wt.% up to 1 bar and 1.2 wt.% up to 8 MPa. After activation, the AC samples presented maximized hydrogen storage capacities of 2.74 wt.% up to 1 bar and 6.6 wt.% up to 8 MPa. The sample AC3 exhibited the highest hydrogen uptake at 1 bar because it had more pores in the range 0.7 to 1 nm, which has been suggested by several authors to be the optimum pore size for hydrogen storage (Rzepka *et al.* 1998; Zhao *et al.* 2011).

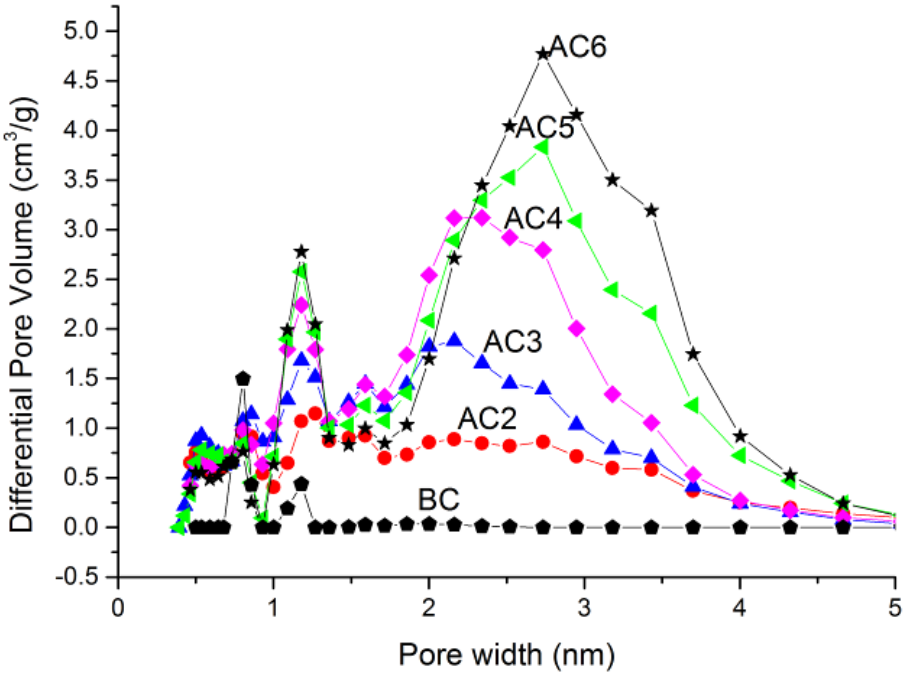

Fig. 8. Pore size distributions from N_2 adsorption-desorption for all the ACs calculated by DFT

The adsorption energy in these pores is much higher compared to that of wider pores surface because of the overlapping of adsorption forces from the opposite walls of the micropores. But the KOH activation is always accompanied of pore widening, so the PSDs shifted to wider pores with higher *W*. The reason why the sample AC5 has the highest hydrogen storage at 4 MPa is first due to the high volume of micropores compared with AC3. And other reason is when the pressure rises, the amount of gas that can be stored by simple compression increases much faster than the adsorbed amount. The contribution of adsorption to total storage thus drops and can even become unfavourable (Zhao *et al.* 2011; Fierro *et al.* 2010).

The hydrogen storage capacities of the lab made sample was also compared with the well-known commercial activated carbon Maxsorb-3 (3203 m^2/g), which is one of the ACs frequently used for hydrogen storage (Ansón *et al.* 2007; Khalil 2013). The Maxsorb-3 was chosen because on one hand they both prepared by activation with alkali hydroxide, on the other hand all the measurements presented in this paper were carried out in the same conditions and same restrictions for equilibrium time. The only difference is the precursor, the lab made sample AC5 used the biomass material bamboo, and the commercial sample maxsorb-3 used the petroleum coke. A comparison of the laboratory-made AC5 with Maxsorb-3, both of which had almost the same surface area, indicated that the developed bamboo ACs exhibited a more appropriate PSD for hydrogen storage at given S_{BET} values, as shown in Fig. 10. Based on the previous findings that hydrogen storage proportional to the surface area, and the latter is clearly not the only factor determining the storage performance; so it can be concluded that the difference of the hydrogen storage performance may due to the fact that the lab made sample had a narrower PSD.

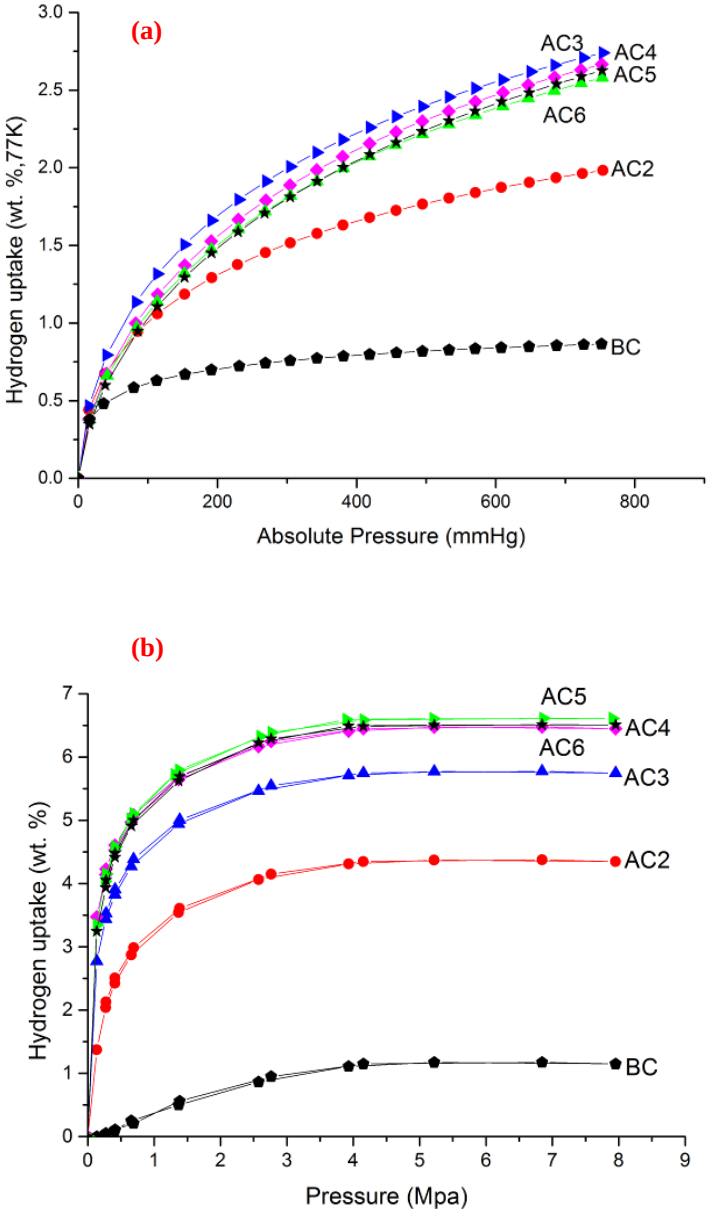

Fig. 9. H_2 storage capacities of the BC and AC samples: (a) at 77 K and up to 8 MPa, and (b) at 77 K and up to 1 bar

Table 3 summarizes the hydrogen adsorption data for AC produced from different sources in the open literature and compared with the super surface area activated carbon prepared in the present study for H_2 adsorption. It can be seen that the activated carbon produced by the bamboo shows that the present experimental results were among the best of the activated carbons from other biomass wastes. Nevertheless, the performance of activated carbon from such sources is also close to that of the other sources. In addition, the hydrogen adsorption obtained in this study was still far from the US DOE target. Thus, a further study should be performed to improve the hydrogen adsorption on activated carbon from bamboo.

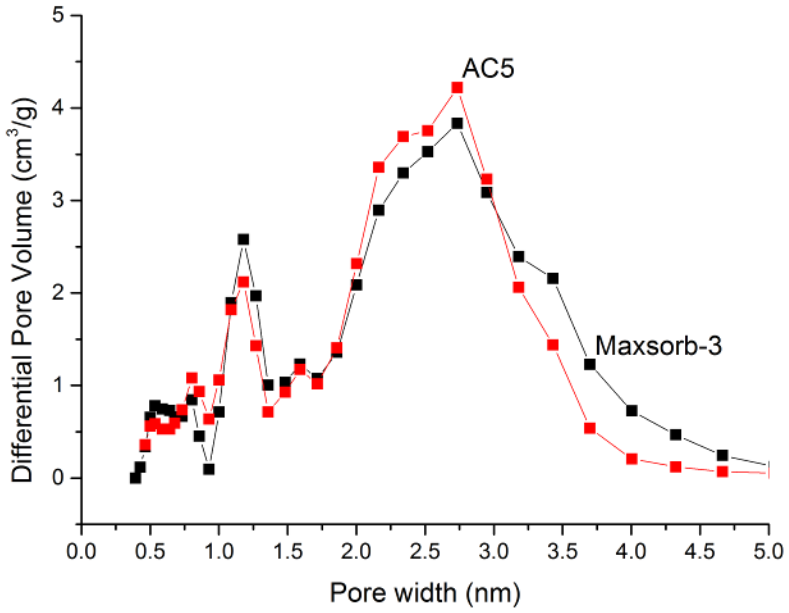

Fig. 10. Pore size distribution of the lab-made sample AC5 and commercial sample of Maxsorb-3

Table 3. Comparison of Activated Carbons by KOH Activation for H_2 Storage

Feedstock	Conditions *T*(K)	Conditions *P*(bar)	Surface area (m^2/g)	H_2 uptake (wt.%)	Ref.
Bamboo	77	40	3208	6.60	This work
	77	1		2.74	
Empty fruit bunch	77	1	687	1.97	Arshad *et al.* 2016
	77	20		2.14	
Anthracites	77	40	3220	6.6	Zhao *et al.* 2014
Rice husk	77	1	3044	2.72	Heo and Park 2015
Chitosan	77	40	3100	5.6	Wróbel-Iwaniec *et al.* 2015
Corncob	77	40	3708	5.8	Wang *et al*. 2014
Activated carbon aerogels	77	20	1980	4.3	Robertson *et al.* 2013
Fungi	77	1	2500	2.4	Wang *et al*. 2014
Activated Carbon Xerogels	77	11	2204	4.3	Zhang *et al.* 2012

CONCLUSIONS

1. A series of super-activated carbons were developed from the biomass material of moso bamboo by means of KOH activation. It was concluded that the developed carbonization and activation processes were able to enhance the microstructures and generate optimal bamboo ACs for hydrogen storage.
2. ACs from bamboo with S_{BET} values as high as 3208 m^2/g and V_{DR} values as high as 1.01 cm^3/g were developed, representing a very promising material for hydrogen storage.

3. The highest hydrogen storage capacities achieved were 6.6 wt.% at 4 MPa and 2.74 wt.% at 1 bar, both at 77 K, which were among the best statistics for hydrogen storage using ACs that have been reported in the literature.
4. The hydrogen storage capacities of the lab-made ACs were much higher than those of the well-known commercial activated carbon Maxsorb-3 due to the optimum pore size achieved by the ACs.

ACKNOWLEDGMENTS

The authors are grateful for the support of the National Natural Science Foundation of China (31300488) and the Fujian Agriculture and Forestry University Fund for Distinguished Young Scholars (xjq201420).

REFERENCES CITED

Ansón, A., Lafuente, E., Urriolabeitia, E., Navarro, R., Benito, A. M., Maser, W. K., and Martínez, M. T. (2007). "Preparation of palladium loaded carbon nanotubes and activated carbons for hydrogen sorption," *J. Alloys Compd.* 436(1-2), 294-297. DOI: 10.1016/j.jallcom.2006.07.026

Arshad, S. H. M., Ngadi, N., Azizb, A. A., Amina, N. S., Jusoha, M., and Wonga, S. (2016). "Preparation of activated carbon from empty fruit bunch for hydrogen storage," *Journal of Energy Storage* 8, 257-261. DOI:10.1016/j.est.2016.10.001

Brunauer, S., Emmet, P. S., and Teller, E. (1938). "Adsorption of gases in multimolecular layers," *J. Am. Chem. Soc.* 60(2), 309-319. DOI: 10.1021/ja01269a023

Choy, K. K. H., Barford, J. P., and McKay, G. (2005). "Production of activated carbon from bamboo scaffolding waste — Process design, evaluation and sensitivity analysis," *Chem. Eng. J.* 109(S1-3), 147-165. DOI: 10.1016/j.cej.2005.02.030

Dubinin, M. M., and Polstyanov, E. F. (1989). "Adsorption properties of carbon adsorbents communication 7. Theoretical analysis of the experimental data on the equilibrium adsorption of vapors of substances on activated charcoals with various microporous structures," *Pure Appl. Chem.* 61(3), 457-467. DOI: 10.1007/BF00849367

Fierro, V., Zhao, W., Izquierdo, M. T., Aylon, E., and Celzard, A. (2010). "Adsorption and compression contributions to hydrogen storage in activated anthracites," *Int. J. Hydrogen Energy*. 35(17), 9038-9045. DOI: 10.1016/j.ijhydene.2010.06.004

Gregg, S. J., and Sing, K. S. W. (1982). *Adsorption, Surface area and Porosity*, 2nd Ed., Academic Press, London, UK. DOI: 10.1149/1.2426447

Heo, Y. J., and Park, S. J. (2015). "Synthesis of activated carbon derived from rice husks for improving hydrogen storage capacity," *J. Ind. Eng. Chem.* 31, 330-334. DOI: 10.1016/j.jiec.2015.07.006

Huang, P. H., Jhan, J. W., Cheng, Y. M., and Cheng, H. H. (2014). "Effects of carbonization parameters of moso-bamboo-based porous charcoal on capturing carbon dioxide," *Scient. World J.* 2014, 937867. DOI: 10.1155/2014/937867

Huang, Y. P., Hou, C. H., Hsi, H. C., and Wu, J. W. (2015). "Optimization of highly microporous activated carbon preparation from moso bamboo using central

composite design approach," *J. Taiwan Inst. Chem. E.* 50, 266-275. DOI: 10.1016/j.jtice.2014.12.019

Khalil, Y. F. (2013). "Experimental determination of dust cloud deflagration parameters of selected hydrogen storage materials: Complex metal hydrides, chemical hydrides, and adsorbents," *J. Loss Prevent. Proc.* 26(1), 96-103. DOI: 10.1016/j.jlp.2012.09.010

Koo, W. K., Gani, N. A., Shamsuddin, M. S., Subki, N. S., and Sulaiman, M. A. (2015). "Comparison of wastewater treatment using activated carbon from bamboo and oil palm: An overview," *J. Trop. Resour. Sustain. Sci.* 3, 54-60.

Li, W., Yang, K., Peng, J., Zhang, L., Guo, S., and Xia, H. (2008). "Effects of carbonization temperatures on characteristics of porosity in coconut shell chars and activated carbons derived from carbonized coconut shell chars," *Ind. Crop. Prod.* 28(2), 190-198. DOI: 10.1016/j.indcrop.2008.02.012

Li, T., Cheng, D. L., Wålinder, M. E. P., and Zhou, D. G. (2015). "Wettability of oil heat-treated bamboo and bonding strength of laminated bamboo board," *Ind. Crop. Prod.* 69, 15-20. DOI: 10.1016/j.indcrop.2015.02.008

Liu, Q. S., Tong, Z., Peng, W., and Liang, G. (2010). "Preparation and characterization of activated carbon from bamboo by microwave-induced phosphoric acid activation," *Ind. Crop Prod.* 31(2), 233-238. DOI: 10.1016/j.indcrop.2009.10.011

Lillo-Ródenas, M. A., Cazorla-Amorós, D., and Linares-Solano, A. (2003). "Understanding chemical reactions between carbons and NaOH and KOH: An insight into the chemical activation mechanism," *Carbon* 41(2), 267-275. DOI: 10.1016/S0008-6223(02)00279-8

Marbán, G., and Valdés-Solís, T. (2007). "Towards the hydrogen economy?" *Int. J. Hydrogen Energy* 32(12), 1625-1637. DOI: 10.1016/j.ijhydene.2006.12.017

Marsh, H., and Rodríguez-Reinoso, F. (2006). "Production and reference material," in: *Activated Carbon*, Elsevier, Oxford, pp. 454-508. DOI: 10.1016/B978-008044463-5/50023-6

Odoemelam, S. A., Onwu, F. K., Uchechukwu, S. C., and Chinedu, M. A. (2014). "Adsorption isotherm studies of Cd(ll) and Pb(ll) ions from aqueous solutions by bamboo-based activated charcoal and bamboo dust," *Am. Chem. Sci. J.* 5(3), 253-269. DOI: 10.9734/ACSJ/2015/14425

Ouyang, X., Jin, R. N., Yang, L. P., Wang, Y. G., and Yang, L. Y. (2014). "Bamboo-derived porous bioadsorbents and their adsorption of Cd(II) from mixed aqueous solutions," *RSC Adv.* 4(54), 28699-28706. DOI: 10.1039/C4RA03422H

Okieimen, C. O., and Ogbeide, S. E. (2009). "The dependence on temperature of carbonization and chemical activation on characteristics of granular activated carbon characteristics," *Adv. Mat. Res.* 62-64, 398-403. DOI: 10.4028/www.scientific.net/AMR.62-64.398

Rango, P. D., Marty, P., and Fruchart, D. (2016). "Hydrogen storage systems based on magnesium hydride: From laboratory tests to fuel cell integration," *Appl. Phys. A Mater. Sci. Process.* 122(2), 1-20. DOI: 10.1007/s00339-016-9646-1

Ren, J., Musyoka, N. M., Langmi, H. W., Swartbooi, A., North, B. C., and Mathe, M. (2015). "A more efficient way to shape metal-organic framework (MOF) powder materials for hydrogen storage applications," *Int. J. Hydrogen Energy* 40(13), 4617-4622. DOI: 10.1016/j.ijhydene.2015.02.011

Robertson, C., and Mokaya, R. (2013). "Microporous activated carbon aerogels via a simple subcritical drying route for CO_2, capture and hydrogen storage," *Micropor. Mesopor. Mat.* 179(17), 151-156. DOI: 10.1016/j.micromeso.2013.05.025

Rzepka, M., Lamp, P., and Casa-Lillo, M. A. D. L. (1998). "Physisorption of hydrogen on microporous carbon and carbon nanotubes," *J. Phys. Chem. B* 102(52), 10894-10898. DOI: 10.1021/jp9829602

Sethia, G., and Sayari, A. (2016). "Activated carbon with optimum pore size distribution for hydrogen storage," *Carbon* 99, 289-294. DOI: 10.1016/j.carbon.2015.12.032

Shang, T. X., Zhang, J., Jin, X. J., and Gao, J. M. (2014). "Study of Cr(VI) adsorption onto nitrogen-containing activated carbon preparation from bamboo processing residues," *J. Wood. Sci.* 60(3), 215-224. DOI: 10.1007/s10086-014-1392-4

Shen, Q., Liu, D. S., Yuan, G., and Ying, C. (2004). "Surface properties of bamboo fiber and a comparison with cotton linter fibers," *Colloids Surf., B* 35(3-4), 193-195. DOI: 10.1016/j.colsurfb.2004.04.002

Stoeckli, F., Slasli, A., Hugi-Cleary, D., and Guillot, A. (2002). "The characterization of microporosity in carbons with molecular sieve effects," *Micropor. Mesopor. Mat.* 51(3), 197-202. DOI: 10.1016/S1387-1811(01)00482-6

Tarazona, P. (1995). "Solid-fluid transition and interfaces with density functional approaches," *Surf. Sci.* 331(331), 989-994. DOI: 10.1016/0039-6028(95)00170-0

Tang, Y., and Smith, G. J. (2014). "A note on Chinese bamboo paper: The impact of modern manufacturing processes on its photostability," *J. Cult. Herit.* 15(3), 331-335. DOI: 10.1016/j.culher.2013.05.004

Vamvuka, D., Troulinos, S., and Kastanaki, E. (2006). "The effect of mineral matter on the physical and chemical activation of low rank coal and biomass materials," *Fuel* 85(12-13), 1763-1771. DOI: 10.1016/j.fuel.2006.03.005

Wang, L. (2012). "Application of activated carbon derived from 'waste' bamboo culms for the adsorption of azo disperse dye: Kinetic, equilibrium and thermodynamic studies," *J. Environ. Manage.* 102, 79-87. DOI: 10.1016/j.jenvman.2012.02.019

Wang, S. Y., Tsai, M. H., Lo, S. F., and Tsai, M. J. (2008). "Effects of manufacturing conditions on the adsorption capacity of heavy metal ions by making bamboo charcoal," *Bioresour. Technol.* 99(15), 7027-7033. DOI: 10.1016/j.biortech.2008.01.014

Wang, R., Amano, Y., and Machida, M. (2013). "Surface properties and water vapor adsorption-desorption characteristics of bamboo-based activated carbon," *J. Anal. Appl. Pyrol.* 104, 667-674. DOI: 10.1016/j.jaap.2013.04.013

Wang, D., Geng, Z., Zhang, C., Zhou, X., and Liu, X. (2014). "Effects of thermal activation conditions on the microstructure regulation of corncob-derived activated carbon for hydrogen storage," *J. Energ. Chem.* 23, 601-608. DOI: 10.1016/S2095-4956(14)60190-X

Wang, J., Senkovska, I., Kaskel, S., Liu, Q. (2014). "Chemically activated fungi-based porous carbons for hydrogen storage," *Carbon*, 75(10), 372-380. DOI: 10.1016/j.carbon.2014.04.016

Wang, Y. X., Ngo, H. H., and Guo, W. S. (2015). "Preparation of a specific bamboo based activated carbon and its application for ciprofloxacin removal," *Sci. Total Environ.* 533, 32-39. DOI: 10.1016/j.scitotenv.2015.06.087

Wróbel-Iwaniec, I., Díez, N., and Gryglewicz, G. (2015). Chitosan-based highly activated carbons for hydrogen storage. *Int. J. Hydrogen Energy* 40(17), 5788-5796.

Wu, J., Xia, H., Zhang, L., Xia, Y., Peng, J., Wang, S., Zheng, Z., and Zhang, S. (2015). "Effect of microwave heating conditions on the preparation of high surface area activated carbon from waste bamboo," *High. Temp. Mat. Pr-Isr.* 34(7), 1-8. DOI: 10.1515/htmp-2014-0096

Xiao, Y., Dong, H., Long, C., Zheng, M., Lei, B., Zhang, H., and Liu, Y. (2014). "Melaleuca bark based porous carbons for hydrogen storage," *Int. J. Hydrogen Energy* 39(22), 11661-11667. DOI: 10.1016/j.ijhydene.2014.05.134

Zhang, J., Yi, G., Liu, Y., Wu, Y., Xiao, Y., and Sun, L. (2012). "KOH-activated carbon xerogels for hydrogen storage," *Chinese Journal of Inorganic Chemistry* 28(12), 2565-2572.

Zhang, J., Shang, T., Jin, X., Gao, J., and Zhao, Q. (2014). "Study of chromium(VI) removal from aqueous solution using nitrogen-enriched activated carbon based bamboo processing residues," *RSC Adv.* 5(1), 784-790. DOI: 10.1039/C4RA11016A

Zhao, W., Fierro, V., Zlotea, C., Aylon, E., Izquierdo, M. T., Latroche, M., and Celzard A. (2011). "Activated carbons with appropriate micropore size distribution for hydrogen adsorption," *Int. J. Hydrogen Energy* 36(9), 5431-5434. DOI: 10.1016/j.ijhydene.2010.12.137

Zhao, W., Fierro, V., Zlotea, C., Izquierdo, M. T., Chevalier-César, C., Latroche, M., and Celzard, A. (2012a). "Activated carbons doped with Pd nanoparticles for hydrogen storage," *Int. J. Hydrogen Energy* 37(6), 5072-5080. DOI: 10.1016/j.ijhydene.2011.12.058

Zhao, W., Fierro, V., Fernández-Huerta, N., Izquierdo, M. T., and Celzard, A. (2012b). "Impact of synthesis conditions of KOH activated carbons on their hydrogen storage capacities," *Int. J. Hydrogen Energy* 37(19), 14278-14284. DOI: 10.1016/j.ijhydene.2012.06.110

Zhao, W., Fierro, V., Fernández-Huerta, N., Izquierdo, M. T., and Celzard, A. (2013). "Hydrogen uptake of high surface area-activated carbons doped with nitrogen," *Int. J. Hydrogen Energy* 38(25), 10453-10460. DOI: 10.1016/j.ijhydene.2013.06.048

Zhao, W., Fan, M., and Gao, H. (2016). "Central composite design approach towards optimization of super activated carbons from bamboo for hydrogen storage," *RSC Adv.* 6(52), 46977-46983. DOI: 10.1039/C6RA06326H

Zhou, G., Meng, C., Jiang, P., and Xu, Q. (2011). "Review of carbon fixation in bamboo forests in China," *Bot. Rev.* 77(3), 262-270. DOI: 10.1007/s12229-011-9082-z

Article submitted: May 19, 2016; Peer review completed: September 23, 2016; Revised version received: December 18, 2016; Accepted: December 27, 2016: Published: January 4, 2017.
DOI: 10.15376/biores.12.1.1246-1262